Canadian Mineralogist
Vol. 24, pp. 329-346 (1986)

A SURVEY OF THE Pd–Pt MINERALIZATION ALONG THE 35-KM STRIKE OF THE J-M REEF, STILLWATER COMPLEX, MONTANA

ALEXIS VOLBORTH
Department of Chemistry and Geochemistry, Montana College of Mineral Science and Technology, Butte, Montana 59701, U.S.A.

MAHMUD TARKIAN
Mineralogy-Petrology Institute, University of Hamburg, Hamburg, West Germany

EUGEN F. STUMPFL
Department of Mineralogy and Petrology, Mining University, 8700 Leoben, Austria

ROBERT M. HOUSLEY
Rockwell International Science Center, Thousand Oaks, California 91360, U.S.A.

ABSTRACT

This investigation of the PGE mineralogy of the J–M Reef in the Stillwater layered complex of Montana is based on cores from several drill-holes covering 35 km of lateral extent. In addition to the main PGE zone, we describe rhenium mineralization in pentlandite–pyrrhotite aggregates associated with michenerite, wehrlite, hessite, chalcopyrite, niccolite, BiNi, cobaltite, magnetite, and major graphite in an underlying graphite–sulfide zone. Grains of PGM, such as vysotskite, braggite, cooperite, moncheite, sperrylite, kotulskite, ferroplatinum, keithconnite, stillwaterite, palladoarsenide, hollingworthite, electrum, and a Cu–Zn–Sn alloy have been selected for electron-microprobe studies. Results include sixty-four analyses and spectral reflectance and VHN microhardness data on Pt-free vysotskite, palladoarsenide, moncheite and Pt–Fe alloys, and comprehensive chemical and optical data on cooperite, braggite and vysotskite. The discovery of rhenium mineralization in graphite-rich coarse pyroxenites under the main PGM zone may indicate a dearth of molybdenum in these deposits. Chlorapatite from these pyroxenites, with up to 6.3% Cl, suggests a role for Cl in a volatile phase; it is this agent that may have caused the separation of Pt from Pd in these deposits.

Keywords; Stillwater Complex, Montana, Pd, Pt, Rh, Ir, graphite–sulfide assemblage, Re, Re_2S_3, vysotskite-braggite, cooperite, palladoarsenide, keithconnite, hollingworthite, Pt–Fe alloys, michenerite, kotulskite, sperrylite, stillwaterite, moncheite, electrum, CuZnFeSn, BiNi, chlorapatite, chlorine.

SOMMAIRE

Ce travail s'adresse à la distribution des minéraux des éléments du groupe du platine dans le banc J–M du massif stratiforme de Stillwater (Montana). L'échantillonage du banc a porté sur les carottes de plusieurs trous de forage le long de son étendue de 35 km. En plus de la zone principale enrichie en éléments du groupe du platine, nous décrivons la minéralisation en rhénium dans les amas de pentlandite et de pyrrhotine associés à: michenerite, wehrlite, hessite, chalcopyrite, niccoline, BiNi, cobaltite, magnétite et graphite majeur dans une zone sous-jacente à graphite + sulfures. Les minéraux suivants ont été étudiés à la microsonde électronique: vysotskite, braggite, cooperite, monchéite, sperrylite, kotulskite, ferroplatine, keithconnite, stillwaterite, palladoarsenide, hollingworthite, électrum et un alliage Cu–Zn–Sn. Nous présentons 64 compositions chimiques et les spectres de réflectance et la dureté de la vysotskite dépourvue de platine, palladoarsenide, monchéite et les alliages Pt–Fe. De plus, nous présentons des données chimiques et optiques complètes pour cooperite, braggite et vysotskite. La découverte d'un enrichissement en rhénium dans les pyroxénites pegmatitiques à graphite audessous de la zone minéralisée principale pourrait indiquer l'absence de molybdène dans ces gisements. La chlorapatite de ces pyroxénites, qui contient jusqu'à 6.3% de chlore, serait un indice d'une phase volatile riche en Cl qui pourrait bien expliquer la séparation des éléments Pt et Pd dans ces gisements.

(Traduit par la Rédaction)

Mots-clés: complexe stratiforme de Stillwater, Montana, Pd, Pt, Rh, Ir, assemblage à graphite + sulfures, Re, Re_2S_3, vysotskite-braggite, cooperite, palladoarsenide, keithconnite, hollingworthite, alliage Pt–Fe, michenerite, kotulskite, sperrylite, stillwaterite, monchéite, électrum, alliage Cu–Zn–Fe–Sn, BiNi, chlorapatite, chlore.

INTRODUCTION

The stratigraphy, petrology and mineralization of some of the Pd–Pt-enriched zones of the Stillwater

Complex in Montana have been described by Todd *et al.* (1982), McCallum *et al.* (1980) and Bow *et al.* (1982). These authors also gave data on the sulfide mineralization and the genesis of the main Pd–Pt zone, called here the J–M Reef. The most recent information on the Stillwater Complex has been compiled in the form of a field guide by Czamanske & Zientek (1985). Page *et al.* (1985) gave a schematic column with locations of sulfide, chromite and PGE mineralization in the Stillwater Complex. The PGE mineralogy of a part of the J–M Reef has been described by Cabri and co-workers based on concentrates, mainly from the West Fork adit (Cabri & Laflamme 1974, Cabri *et al.* 1975, 1976, 1977, 1979, Cabri 1981). Mineralization within the J–M Reef stretches for about 35 km as an almost continuous, 1- to 3-m-wide band, stratigraphically situated in the lower part of the 4000-m thick Banded Series, in the middle of a 120-m wide Troctolite–Anorthosite Zone (Todd *et al.* 1982). The sulfides occur mainly between two somewhat discontinuous olivine-bearing peridotite members; they are concentrated in a troctolite layer, but occur commonly also in relatively pure anorthosite on both sides of the troctolite, as well as in the peridotite and locally in the gabbroic rocks below. The nature of the distribution of the sulfides in the J–M Reef is shown by Todd *et al.* (1982, Fig. 6, p. 1464). These authors show how the sulfide mineralization in the J–M Reef alternates within and between anorthosite, troctolite, peridotite, and the underlying two-pyroxene gabbro and even the norite. The main sulfides of the reef are pentlandite, pyrrhotite and chalcopyrite. The other common sulfides are pyrite, millerite, cubanite and violarite. Wolfgram & Evans (1980) found that an immiscible, high-temperature, monosulfide solid-solution of Ni, Cu, Fe and S evolved at about 250°C into the three-phase assemblage pentlandite – pyrrhotite – chalcopyrite. They emphasized that pentlandite occurs as quite coarse grains and is commonly concentrated in the central parts of the three-phase aggregates. Widespread globules and roundish inclusions of sulfides in the silicates indicate, however, a high-temperature origin. These authors described a discontinuous rim of chalcopyrite and a complex intergrowth of chalcopyrite with pentlandite. The appearance of millerite as a replacement of pyrrhotite is attributed to the release of Ni during the widespread serpentinization of olivine. Locally, strong oxidation has produced magnetite replacing the sulfides. Todd *et al.* (1982) found that the sulfides tend to aggregate into larger clots in the lower part of the reef, to form net textures in the middle and to be disseminated near its top. Page (1971, 1979) has described sulfides from the Basal Series and the chromitite layers of the Stillwater Complex.

THE BASE-METAL SULFIDES AND THEIR TEXTURES

According to our observations, the sulfides occur in different generations, mainly interstitially between the cumulus crystals. In addition, they form complex, irregularly shaped aggregates, mostly between 1 and 5 mm across, but may attain several centimetres in diameter. They also tend to form net-like structures that engulf some cumulus crystals completely, as well as disseminated, small, interstitially located and variably shaped, mostly complex grains. These primary, disseminated sulfides are not to be confused with the secondary disseminated sulfides, which occur in minute, mostly monomineralic angular grains with biotite intergrowths in serpentinized, bastitized and "amphibolized" grains of pyroxene and olivine, and also in epidotized plagioclase. The main sulfide mineral replacing the silicates is chalcopyrite. However, this replacement occurs mainly as a rim on aggregates of primary sulfides. Clear preference in such replacement for intercumulus and oikocrystic pyroxene is observed. Serpentinized olivine (olivine is the most completely decomposed mineral in these rocks) is also the preferred host for such microscopic disseminations of sulfides. There are areas where the dominant secondary sulfides consist of pyrrhotite and pentlandite, as well as pyrite, which appears in most cases as the latest sulfide,

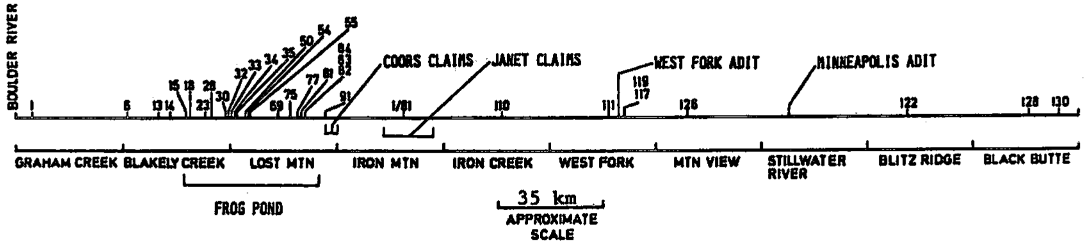

FIG. 1. Lateral distribution of drill cores along the J–M Reef, with location of polished sections studied.

generally forming dendrite-like stringers and chains that seem to criss-cross locally and replace the other sulfides. This pyrite is idiomorphic and has a tendency to replace even fresh plagioclase crystals in cumulates, and it occasionally rims these early grains and penetrates into their centres. Another typical phenomenon of replacement, especially common in exceptionally high-grade ore, is the appearance of laminar replacement-textures in pyrrhotite; thin parallel lamellae of magnetite are intercalated with fine aggregates of pyrite and marcasite with occasional euhedral crystals of nickeloan pyrite. Such a pattern of replacement has been described by Genkin *et al.* (1981) from Noril'sk. Ilmenite and hematite lamellae occur in this mixture. In the vicinity of pentlandite, in these aggregates, a considerable amount of violarite quite commonly forms in the sulfide lamellae surrounded by pyrite and marcasite. This replacement generally extends into the pentlandite, in which case violarite can be quite abundant. Bornite may become abundant in pyroxene-rich regions.

Flakes and minute grains of mackinawite are widespread, mainly in serpentinized olivine but also in altered pyroxene. In strongly serpentinized regions, fine-grained graphite may be found in veinlets. Where intermixed with fine marcasite and mackinawite in such veinlets, the recognition of individual mineral grains of these minerals is very difficult. In altered regions, in addition to millerite, we also find heazlewoodite.

Volborth & Housley (1983, 1984) and Volborth (1984, 1985) have recently described pegmatoid, graphite-rich pyroxenites that occur about 100 to 200 metres below the J–M Reef in a yet poorly defined zone; the pyroxenites carry similar sulfide mineralization, but much lower amounts of the PGE and infrequent PGM. These pegmatoid pyroxenites are characterized by a much higher Pt/Pd ratio (1:1 *versus* 1:4 in the reef) and carry unusual concentrations of Re and a Re-sulfide. They probably represent an important late-stage development of Pd–Pt mineralization within the Stillwater Complex. In the graphite-rich pegmatoid pyroxenites, in addition to the other typical ore-minerals, nickeline and other Ni and Co arsenides are common, whereas in the reef they are quite rare. Of importance are the occurrence of significant chlorine in most of the graphite and the presence of almost end-member chlorapatite detected by us. Chlorine data on the apatite and the graphite are given below following the account on michenerite.

THE PLATINUM-GROUP MINERALS

The distribution of the PGM in relation to the main sulfides and the development of the sulfide-silicate textural relationships have been described by Bow *et al.* (1982, p. 1490-1491). According to these authors, the early sulfide liquids were originally trapped interstitially in olivine cumulates and as droplets in the olivine. Progressive resorption of olivine, increased dominance of bronzite and a more complex mineralogy caused further growth of the entrapped sulfide aggregates; there was a tendency for some small PGM grains, such as vysotskite, to form. Further crystallization tended to segregate the chalcopyrite outward, so that it commonly forms a rim around the sulfide aggregates. Late-stage sulfur saturation seems to be indicated by the appearance of pyrite replacing the pentlandite and pyrrhotite. Bow *et al.* (1982), as well as Todd *et al.* (1982, p. 1472-1473), emphasized the small grain-size of the PGM and their close association with sulfide aggregates, especially along their rims and in the chalcopyrite veinlets emanating from these rims. A somewhat erratic and clustered distribution of the PGM seems to be the rule, especially in the pegmatoid portions. Morphology and composition of the PGM appear to reflect the composition of the host rock to some degree.

Of interest are the findings by Boudreau & McCallum (1984) of nine other Pd–Pt-poor sulfide zones in the Banded series, of which the richest, the Picket Pin Pt–Pd zone, carries lower concentrations of the PGE, by two orders of magnitude, than the J–M Reef.

The dominant PGM, according to Cabri (1981) and the above authors, are braggite–vysotskite, moncheite, cooperite, sperrylite, kotulskite and Pt–Fe alloys (see also Conn 1979). The frequency of a particular PGM seems to vary depending on location (Todd *et al.* 1982). Cabri and coworkers, as well as Todd *et al.* (1982), have published results of numerous electron-microprobe analyses of the Stillwater PGM. Presently, 31 noble-metal minerals are known.

Metallic phases: platinum, Pt; Pt–Fe alloys, Pt_3Fe; rhodian platinum, (PtRh); platinian rhodium, (Rh, Pt); rhodium, Rh; palladian gold (Au,Pd); gold, Au; electrum, (Au,Ag); silver, Ag. *Sulfides:* braggite, (Pt,Pd)S; cooperite, PtS; vysotskite, PdS; laurite, RuS_2. *Tellurides:* moncheite, $PtTe_2$; kotulskite, PdTe; merenskyite, $PdTe_2$; telluropalladinite, Pd_5Te_2; keithconnite, $Pd_{3-x}Te$; michenerite, PdBiTe; temagamite, Pd_3HgTe_3; hessite, Ag_2Te. *Arsenides:* sperrylite, $PtAs_2$; stillwaterite, Pd_8As_3; palladoarsenide, Pd_2As; palladobismutharsenide, $Pd_{10}As_4Bi$; hollingworthite, RhAsS; arsenopalladinite, $Pd_8As_{2.5}Sb_{0.5}$. *Antimonides:* mertieite II, Pd_8Sb_3. *Stannides and plumbites:* rustenburgite, $(Pt,Pd)_3Sn$; plumbopalladinite, Pd_3Pb_2; zvyagintsevite, Pd_3Pb. In addition, about 17 analyzed noble-metal minerals have been detected, including new minerals. Of these, most are palladium minerals, and many may be varieties.

There are few previous ore-microscope studies of the PGM in the Stillwater Reef that are supported by electron-microprobe (EMP) and scanning-electron microscope analyses. These are mainly based on concentrates from the West Fork adit (Cabri & Laflamme 1974, Cabri *et al.* 1975, 1976, 1977, 1979, Cabri 1981), and on two cores from the Dead Tree area west of Frog Pond adit (Todd *et al.* 1982, who

TABLE 1. COMPILATION OF MINERALOGICAL DATA PER DRILL-CORE ALONG THE J-M REEF FROM WEST TO EAST

Pol. sect. No.	1-84	6-84	13-84	14-84	15-84	16-84	18-84	23-84
Location	Graham Creek	Blakely Creek	Blakely Creek	Blakely Creek	Frog Pond (Blakely Cr.)	Frog Pond (Blakely Cr.)	Frog Pond (Blakely Cr.)	Frog Pond (Blakely Cr.)
Depth, feet	31.7-31.9	330.0-330.5	88.0-88.4	131.6-131.8	521.0-521.2	531.0-531.2	90.7-91.0	487.7-488.0
Rock type	poC ?	pC, pegm.	pobC, ?	pC ?	pabC ?	pC	pbC	poC-pobC
Alteration		FRESH	OLIV. SERP.	SERPENTINIZED	SERPENTINIZED		SERP., EPIDOT.	OLIV. SERP.
Pt/Pd ratio	(1:3.7)		(1:2.9)					
Pt-Pd, Rh,Au minerals semiquant. + microsc.	MONCHEITE COOPERITE	SPERRYLITE	MONCHEITE VYSTOSKITE KEITHCONNITE GOLD	MONCHEITE (Au,Ag) Pt-Fe HOLLING-WORTHITE	SPERRYLITE MONCHEITE VYSOTSKITE BRAGGITE PALLADO-ARSENIDE	SPERRYLITE KOTULSKITE STILLWATERITE	KOTULSKITE ?	MONCHEITE Pt-Fe
Pt-Pd, Rh,Au minerals analyzed		SPERRYLITE	KEITHCONNITE	HOLLING-WORTHITE	PALLADO-ARSENIDE STILLWATERITE	SPERRYLITE	INCOMPLETE	MONCHEITE Pt-Fe
Pd in pentlandite	0.1	0.1	0.1-0.4			1.07		
Sulfide minerals detected etc.	PENTLANDITE PYRRH. CP., PYR. SPHALERITE BRAVOITE	PENTLANDITE PYRRH. CP., PYR., BRAVOITE MILLERITE GALENA HEMATITE MAGNETITE SPHALERITE	PENTLANDITE PYRRH., CP. PYR. MAGNETITE-MESH ILMENITE CHROMITE	PENTLANDITE PYRRH., CP. PYR. SPHALERITE CoAsS	PENTLANDITE PYRRH., CP. PYR. BRAVOITE	PENTLANDITE PYRRH., CP. PYR.	PENTLANDITE PYRRH., CP. MILLERITE HEAZLEWOODITE?	PENTLANDITE PYRRH., CP. MAGNETITE-MESH
Reflectance			KEITHCONNITE		PALLADOARSENIDE			Pt-Fe
Hardness meas.					PALLADOARSENIDE			

Pol. sect. No.	28-84	30-84	32-84	33-84	34-84	35-84	50-84	54-84
Location	Frog Pond (Blakely Cr.)	Frog Pond (Blakely Cr.)	Frog Pond (Blakely Cr.)	Frog Pond (Blakely Cr.)	Frog Pond (Blakely Cr.)	Frog Pond (Blakely Cr.)	Frog Pond (Lost Mtn.)	Frog Pond (Lost Mtn.)
Depth, feet	963.0-963.6	796.0-796.2	70.5-70.7	49.0-49.1	830.8-831.0	833.5-833.9	1530.2-1530.6	1536.8-1537.0
Rock type	poC	poC, pegm.	pbC, pegm.	pobC	pC-pbC	poC, pegm.	pbC	pC
Alteration	SERPENTINIZED	OLIV. SERP.	OLIV. SERP.	FRESH	OLIV. SERP.	FRESH	FRESH	FRESH
Pt/Pd ratio			(1:2.8)				(1:3.1:3.5,1:4.1)	
Pt-Pd, Rh,Au minerals semiquant. + microsc.	MONCHEITE Pt-Fe COOPERITE BRAGGITE (Au,Ag)	MONCHEITE Pt-Fe BRAGGITE COOPERITE	MONCHEITE COOPERITE BRAGGITE	MONCHEITE Pt-Fe	MONCHEITE	MONCHEITE	MONCHEITE COOPERITE BRAGGITE SPERRYLITE	MONCHEITE BRAGGITE (Au,Ag)
Pt-Pd, Rh,Au minerals analyzed	MONCHEITE Pt-Fe (Au,Ag) COOPERITE	MONCHEITE COOPERITE Pt-Fe	MONCHEITE COOPERITE BRAGGITE Pt-Fe	MONCHEITE Pt-Fe	MONCHEITE	MONCHEITE	COOPERITE BRAGGITE	BRAGGITE
Pd in pentlandite								1.4
Sulfide minerals detected etc.	PENTLANDITE PYRRH., CP. MARCASITE MAGNETITE-MESH GRAPHITE	PENTLANDITE PYRRH. CP. CHROMITE	PENTLANDITE PYRRH. CP. MAGNETITE	PENTLANDITE PYRRH., CP. MILLERITE	PENTLANDITE PYRRH., CP. MILLERITE MARCASITE MAGNETITE-MESH MACKINAWITE GRAPHITE	PENTLANDITE PYRRH., CP. PYR. CUBAN. MILLERITE HEAZLEWOODITE MACKINAWITE	PENTLANDITE PYRRH., CP. PYR.	PENTLANDITE PYRRH., CP. PYR. SPHALERITE
Reflectance	Pt-Fe	Pt-Fe MONCHEITE COOPERITE	BRAGGITE MONCHEITE COOPERITE	MONCHEITE Pt-Fe	MONCHEITE	MONCHEITE		
Hardness meas.	Pt-Fe	MONCHEITE	MONCHEITE COOPERITE			MONCHEITE		

reported 12 new compositions of PGM), as well as on the cores from the pegmatoid pyroxenite of the Janet-50 claims (Volborth & Housley 1983, 1984). To our knowledge, no comprehensive ore-microscope study supported by EMP and SEM of the whole length of the mineralized zone exists. We attempt therefore to give an overview of the 35 km of the J-M Reef.

For this work, out of some 300 available drill holes, about 70 cores with the highest assay-values were selected. A total of 140 polished sections were made and examined in reflected light at magnifica-

Pol. sect. No.	55-84	69-84	75-84	77-84	81-84	82-84	83-84	91-84
Location	Frog Pond (Lost Mtn.)	Frog Pond (Lost Mtn.)	Frog Pond (Lost Mtn.)	Frog Pond (Lost Mtn.)	Frog Pond (Lost Mtn.)	Frog Pond (Lost Mtn.)	Frog Pond (Lost Mtn.)	Lost Mtn.
Depth, feet	1822.0-1822.3	286.5-287.0	1295.6-1296.0	415.4-415.5	635.2-636.0	91.3-91.7	92.0-92.8	270.2-270.4
Rock type	pC	OLIV. GABBRO	pC	OLIV. GABBRO	poC	pbC	pbC	pC
Alteration	FRESH	FRESH ?	SERPENTINIZED		SERPENTINIZED	FRESH	FRESH	FRESH
Pt/Pd RATIO		1:4.2 (6 ft)				1:3.8 (10 ft)	1:3.8 (10 ft)	
Pt-Pd, Rh,Au Minerals SEMIQUANT. + MICROSCOPE	SPERRYLITE BRAGGITE	MONCHEITE BRAGGITE	SPERRYLITE MONCHEITE Pt-Fe COOPERITE (Au,Ag)	MONCHEITE VYSOTSKITE	MONCHEITE Pt-Fe	INCOMPLETE	MONCHEITE Pt-Fe (Au,Ag)	MONCHEITE SPERRYLITE BRAGGITE VYSOTSKITE PALLADOARSENIDE
Pt-Pd, Rh,Au Minerals ANALYZED	BRAGGITE	MONCHEITE (Cu,Zn,Sn)	SPERRYLITE	MONCHEITE			PURE $PtTe_2$	PALLADOARSENIDE SPERRYLITE
Pd IN PENTLANDITE	0.2			3.4				
Sulfide Minerals DETECTED ETC.	PENTL., PYRRH. CP., PYR. MILLERITE MARCASITE VIOLARITE HEAZLEWOODITE SPHALERITE	PENTL., PYRRH. CP., PYR. TETRAHEDRITE CUBANITE MARCASITE Cu	PENTL., PYRRH. CP., PYR. NICCOLITE	PENTL. PYRRH., CP. PYR. SPHALERITE MILLERITE MARCASITE MAGNETITE HEMATITE	PENTL., PYRRH. CP., PYR.	PENTL.,PYRRH. CP., PYR.	PENTL. PYRRH., CP. PYR. SPHENE	PENTL., PYRRH. CP., PYR. MARCASITE
Reflectance								
Hardness meas.								

Pol. sect. No.	1-81	110-84	111-84	117-84	119-84	122-84	126-84	130-84
Location	Iron Mtn.	Iron Creek	West Fork	West Fork	West Fork	Blitz Ridge	Mtn. View	Black Butte
Depth, feet	250.9-251.0	208.4-208.6	236.5-236.8	244.5-244.8	247.6-247.9	65.0-65.3	282.8-283.0	93.2-95.5
Rock type	pabC	pC	pobC	pC	pbC	pC	obC	pC
Alteration		FRESH		SERP., EPIDOT.		FRESH		FRESH
Pt/Pd RATIO	(1:3.1; 1:2.9)							(1:2.8)
Pt-Pd, Rh,Au Minerals SEMIQUANT. + MICROSCOPE	VYSOTSKITE BRAGGITE	INCOMPLETE	INCOMPLETE	VYSOTSKITE COOPERITE MONCHEITE	BRAGGITE MONCHEITE SPERRYLITE	INCOMPLETE	VYSOTSKITE BRAGGITE Pt-Fe MONCHEITE	SPERRYLITE MONCHEITE
Pt-Pd, Rh,Au Minerals ANALYZED	VYSOTSKITE BRAGGITE			COOPERITE VYSOTSKITE MONCHEITE	BRAGGITE COOPERITE		VYSOTSKITE	
Pd IN PENTLANDITE					0.6			
Sulfide Minerals DETECTED ETC.	PENTL., PYRRH. CP., PYR. MILLERITE MAGNETITE	PENTL. PYRRH. CP.	PENTL. PYRRH. CP.	PENTL.,PYRRH. CP., PYR. SPHALERITE ILMENITE	PENTL., PYRRH. CP., PYR. ILMENITE	PENTL. PYRRH. PYR. CP.	PENTL., PYRRH. CP., PYR MILLERITE BORNITE CUBANITE COVELLITE ILMENITE MAGNETITE	PENTL., PYRRH. CP.,PYR.
Reflectance	VYSOTSKITE						VYSOTSKITE	
Hardness meas.	VYSOTSKITE							

Abbreviations used in Table 1: pc plagioclase cumulate, poC plagioclase olivine cumulate, pboC plagioclase bronzite olivine cumulate, pabC plagioclase augite bronzite cumulate, pbC plagioclase bronzite cumulate, pobC plagioclase olivine bronzite cumulate, obC olivine bronzite cumulate, oliv. serp. olivine only is serpentinized, serp. whole rock is serpentinized, epidot. rock is epidotized, pyrrh. pyrrhotite, cp chalcopyrite, pyr. pyrite, sph sphalerite, pentl. pentlandite.

TABLE 2A. COMPOSITION OF PG MINERALS ALONG THE J-M REEF

MINERAL	No.	Pt	Pd	Fe	Te	Bi	As	SUM	REMARKS	FORMULA
Moncheite	23/84	42.7	0.0	0.2	57.2			100.9	0.7%Ni	$(Pt_{0.96}Ni_{0.06}Fe_{0.01})Te_{1.97}$
Moncheite	23/84-1	42.1	0.0	0.04	57.2	0.8		100.1		$(Pt_{0.97}Fe_{<0.01})(Te_{2.00}Bi_{0.02})$
Moncheite	23/84-4	42.1	0.0	0.3	57.0	1.6		101.1		$(Pt_{0.96}Fe_{0.02})(Te_{1.98}Bi_{0.04})$
Moncheite	28/84-3	42.1	0.0		56.7	1.2		100.0		$Pt_{0.97}(Te_{2.00}Bi_{0.03})$
Moncheite	30/84-4	42.1	0.0	0.1	56.7	1.1		100.1		$(Pt_{0.97}Fe_{<0.01})(Te_{2.00}Bi_{0.02})$
Moncheite	30/84-6	43.4	0.06	0.3	55.9			99.8	0.1%Ni	$(Pt_{1.00}Pd_{<0.01}Fe_{0.02}Ni_{0.01})Te_{1.97}$
Moncheite	32/84-3	42.2	0.0	0.04	57.5	0.3		100.0		$(Pt_{0.97}Fe_{<0.01})(Te_{2.02}Bi_{<0.01})$
Moncheite	32/84-6	42.0	0.0		57.6	0.7		100.3		$Pt_{0.96}(Te_{2.02}Bi_{0.02})$
Moncheite	33/84-2	43.0	0.0		57.7	0.3		100.9		$Pt_{0.98}(Te_{2.01}Bi_{<0.01})$
Moncheite	34/84-3	41.3	0.01		53.3	5.8		100.7	0.2%Sb	$Pt_{0.96}(Te_{1.90}Bi_{0.13}Sb_{<0.01})$
Moncheite	34/84-6	41.5	0.3		57.2	0.8		100.1	0.3%Sb	$(Pt_{0.95}Pd_{<0.01})(Te_{2.01}Bi_{0.02}Sb_{<0.01})$
Moncheite	34/84-6	42.5	0.1	0.3	56.8			99.8	0.1%Ni	$(Pt_{0.98}Fe_{0.02}Pd_{<0.01}Ni_{<0.01})Te_{1.99}$
Moncheite	35/84-2	41.6	0.2		56.4	1.4		99.9	0.3%Sb	$(Pt_{0.96}Pd_{0.01})(Te_{1.99}Bi_{0.03}Sb_{0.01})$
Moncheite	35/84-1	42.5	0.0		56.0	1.9		100.7	0.3%Sb	$Pt_{0.98}(Te_{1.97}Bi_{0.04}Sb_{<0.01})$
Moncheite	69/84-12a	42.5		0.7	55.0			98.2		$(Pt_{0.99}Fe_{0.06})Te_{1.95}$
Moncheite	77/84-6	42.8		0.3	54.8	0.9		99.1	0.4%Sb	$(Pt_{0.99}Fe_{0.02})(Te_{1.95}Bi_{0.02}Sb_{0.02})$
Moncheite	77/84-8	41.9		0.3	55.0	0.8		98.3	0.4%Sb	$(Pt_{0.98}Fe_{0.02})(Te_{1.97}Bi_{0.02}Sb_{0.01})$
Moncheite	117/84-16a	41.6			56.3	0.4		98.5	0.3%Sb	$Pt_{0.97}(Te_{2.01}Sb_{0.01}Bi_{0.01})$
Sperrylite	6/84-1	57.4		0.1			43.3	101.5	0.7%S	$(Pt_{0.99}Fe_{0.01})(As_{1.94}S_{0.06})$
Sperrylite	15/84-4-A$_1$	57.4	0.1				41.7	99.1		$(Pt_{1.03}Pd_{<0.01})As_{1.96}$
Sperrylite	15/84-3	58.3					41.8	100.1		$Pt_{1.05}As_{1.95}$
Sperrylite	15/84-1A	57.5					42.8	100.3		$Pt_{1.02}As_{1.98}$
Sperrylite	15/84-3	57.1	0.1	0.4			41.0	100.1	0.8%Ni 0.8%S	$(Pt_{0.99}Ni_{0.04}Fe_{0.02}Pd_{<0.01})(As_{1.86}S_{0.08})$
Sperrylite	91/84-3b	55.7	1.3	0.9			42.4	100.3		$(Pt_{0.98}Pd_{0.04}Fe_{0.05})As_{1.93}$
Stillwaterite	15/84-3A		79.0				20.8	99.8		$Pd_{8.00}As_{3.00}$
Kotulskite	16/84-2y		43.6	2.7	46.3	6.0		100.0	1.4%Ni	$(Pd_{0.94}Fe_{0.11}Ni_{0.05})(Te_{0.83}Bi_{0.07})$
Keithconnite	13/84-3		67.3		29.9	0.8		98.0		$Pd_{2.65}(Te_{0.98}Bi_{0.02})$
Palladoarsenide	15/84-4-A$_2$	0.0	75.2				25.3	100.5		$Pd_{2.03}As_{0.97}$
Palladoarsenide	91/84-3a	0.03	75.0	0.3			24.7	100.0		$(Pd_{2.035}Fe_{0.015})As_{0.95}$
Michenerite	C-32/AV		24.6	1.5	28.4	48.1		102.6	Janet-50	$(Pd_{1.04}Fe_{0.12})(Bi_{1.03}Te_{1.00})$

TABLE 2B. COMPOSITION OF PG MINERALS ALONG THE J-M REEF

MINERAL	No.	Pt	Pd	Ni	Fe	S	SUM	FORMULA
Cooperite	28/84-10	77.3	4.7	0.9	0.5	14.8	98.3	$(Pt_{0.85}Pd_{0.1}Ni_{0.03}Fe_{0.02})S_{1.00}$
Cooperite	30/84-2B	85.4	0.8	0.7	0.4	12.8	100.1	$(Pt_{1.01}Pd_{0.02}Ni_{0.02}Fe_{0.02})S_{0.93}$
Cooperite	30/84-6	82.7	0.8	1.2	0.8	13.6	99.1	$(Pt_{0.95}Ni_{0.05}Pd_{0.01}Fe_{0.03})S_{0.96}$
Cooperite	32/84-7	76.6	8.0	0.7	0.8	13.9	100.0	$(Pt_{0.85}Pd_{0.16}Ni_{0.02}Fe_{0.03})S_{0.94}$
Cooperite	50/84-3	81.7	2.4	1.5	0.05	14.4	100.1	$(Pt_{0.91}Ni_{0.05}Pd_{0.05}Fe_{0.01})S_{0.98}$
Cooperite	117/84-15	82.4		1.1		14.3	97.8	$(Pt_{0.95}Ni_{0.04})S_{1.01}$
Cooperite	119/84-1x	72.8	2.3	7.1	0.3	16.4	98.8	$(Pt_{0.73}Ni_{0.23}Pd_{0.05}Fe_{0.01})S_{0.99}$
Braggite	32/84-9	54.0	20.7	5.2	0.5	19.4	99.8	$(Pt_{0.47}Pd_{0.33}Ni_{0.15}Fe_{0.02})S_{1.03}$
Braggite	50/84-5	17.7	48.7	11.4		24.1	101.9	$(Pd_{0.61}Ni_{0.26}Pt_{0.12})S_{1.01}$
Braggite	54/84-8	39.2	32.6	8.8		21.4	102.0	$(Pd_{0.46}Pt_{0.30}Ni_{0.23})S_{1.01}$
Braggite	55/84	33.2	38.8	7.2	0.5	21.7	101.4	$(Pd_{0.55}Pt_{0.25}Ni_{0.18}Fe_{0.01})S_{1.01}$
Braggite	1/81-3	18.3	48.0	10.6		23.6	100.6	$(Pd_{0.62}Ni_{0.25}Pt_{0.13})S_{1.00}$
Braggite	1/81-4	46.6	30.2	5.0		19.9	102.6	$(Pd_{0.46}Pt_{0.40}Ni_{0.14})S_{1.00}$
Braggite	1/81-8	64.9	14.7	5.4		18.0	103.0	$(Pt_{0.59}Pd_{0.24}Ni_{0.16})S_{1.01}$
Braggite	119/84-1	44.0	25.7	10.3	0.1	20.3	100.4	$(Pd_{0.38}Pt_{0.35}Ni_{0.27}Fe_{0.01})S_{1.00}$
Vysotskite	54/84-7b	7.7	56.1	12.3		24.7	100.8	$(Pd_{0.68}Ni_{0.27}Pt_{0.05})S_{1.00}$
Vysotskite	1/81-1	0.3	64.7	11.1		25.2	101.3	$(Pd_{0.76}Ni_{0.24}Pt_{0.01})S_{0.99}$
Vysotskite	1/81-2	8.3	58.5	10.6		24.6	102.0	$(Pd_{0.71}Ni_{0.23}Pt_{0.05})S_{1.01}$
Vysotskite	117/84-6	0.0	61.0	13.2		24.6	98.8	$(Pd_{0.73}Ni_{0.28})S_{0.98}$
Vysotskite	126/84-1	0.0	67.4	7.3	0.6	24.7	100.0	$(Pd_{0.82}Ni_{0.16}Fe_{0.01})S_{1.01}$
Vysotskite	126/84-7b	0.1	62.8	9.8	0.4	24.4	97.5	$(Pd_{0.77}Ni_{0.22}Fe_{0.01})S_{1.00}$
Pt-Fe	23/84-3	86.5	2.8	0.4	10.9		100.6	$(Pt_{0.66}Pd_{0.04}Fe_{0.29}Ni_{0.1})$
Pt-Fe	28/84-2	88.8	2.6		9.9		101.3	$(Pt_{0.69}Pd_{0.04}Fe_{0.27})$
Pt-Fe	28/84-10	87.7	2.8	0.3	10.6		101.4	$(Pt_{0.67}Pd_{0.04}Fe_{0.28}Ni_{0.01})$
Pt-Fe	30/84-3	85.4	4.8	0.1	10.7		100.9	$(Pt_{0.65}Pd_{0.06}Fe_{0.28}Ni_{0.01})$
Pt-Fe	30/84-2A	88.2	3.0	0.3	10.5		101.9	$(Pt_{0.67}Pd_{0.04}Fe_{0.28}Ni_{0.01})$
Pt-Fe	30/84-6	85.9	3.0	0.6	10.8		100.2	$(Pt_{0.66}Pd_{0.04}Fe_{0.29}Ni_{0.01})$
Pt-Fe	32/84-2	93.0	0.1	0.2	9.6		102.8	$(Pt_{0.73}Pd_{0.01}Fe_{0.26}Ni_{0.01})$
Pt-Fe	33/84-3	91.2	0.4		10.2		101.7	$(Pt_{0.71}Pd_{0.01}Fe_{0.28})$
Pt-Fe	33/84-2	87.4	1.0		9.9		98.3	$(Pt_{0.71}Pd_{0.01}Fe_{0.28})$
Pt-Fe	33/84-1	86.6	4.0		11.3		101.8	$(Pt_{0.65}Pd_{0.05}Fe_{0.30})$

tions of up to 500× in oil immersion, and about 40 sections with optically suspected Pd–Pt minerals were picked out. From these, interesting grains of between 5 to 200 micrometres in diameter were selected for EMP analyses, which were performed with three instruments: the 1984–85 Model Camebax Microbeam CD by Cameca and the ARL–EMX–SM in Hamburg, and the ARL–SEMQ in Leoben. The measurements of Vickers hardness (VHN) were performed on the analyzed grains with a Leitz Durimet with an accuracy ± 30 kg/mm^2. The measurements of spectral reflectance were done using the Zeiss microphotometer MPM and a WTiC standard, as described by Tarkian & Bernhardt (1984). The accuracy of measurements is within ± 1.5% (relative). A single filter for 16 wavelengths between 400 and 700 nm, with a half-width of ± 6 nm, has been used as monochromator.

We have analyzed 64 of the larger grains of PGM and noble-metal-alloy grains and have recorded the results in the west-to-east sequence with other mineralogical data (Table 1). The location of the polished sections and the drill cores is shown in Figure 1. Further, we have tabulated the chemical composition of the minerals in Tables 2A and 2B in the same sequence. In Table 1, mineralogical and other data are compiled on 32 drill cores, starting with the westernmost drill-hole and proceeding toward the east. The position of polished core segments is given in feet with a precision of about ± 0.1 feet, to facilitate exact location of the material studied. To enable later additions as future work progresses, even incomplete data on the cumulate rock-type and mineralogical association are given. The small size of most samples commonly has made it impossible to use the terminology of cumulates used by Todd *et al.* (1982) with certainty. Where a value of the ratio Pt/Pd could be calculated, it is given. This part is very incomplete and is being presently extended. It is important to note that Pt/Pd varies considerably and increases to 1:1 in the graphite-pyroxenite zone below the J–M Reef. The optically detected and, in most cases, qualitatively (SEM, EMP) analyzed Pt, Pd, Rh and Au minerals are listed. In a separate row, the quantitatively analyzed noble-metal minerals are listed again. The latter compositions appear in Tables 2A and 2B. The data on Pd in pentlandite are quite incomplete, but because of their importance, they are listed where available. Sulfide and other ore minerals, mainly of base metals and identified mostly in reflected light, with EMP qualitative checks, are listed further down the columns. Noble-metal minerals on which optical, reflectance and hardness measurements were performed are listed again in the last two rows under "reflectance" and "hardness meas." We attempt to list the minerals in sequence of abundance.

Mineral assemblages in the immediate vicinity of the analyzed grains and related textural features were noted. An attempt was made to evaluate the degree of alteration, because the nature of mineralization appears to be influenced more by processes of alteration than by rock type. We were able to distinguish several grades of alteration or replacement:

1. Fresh, relatively unaltered rock with remnants of unaltered olivine, fresh unaltered pyroxenes, and clear plagioclase. No significant serpentine, secondary amphiboles, or epidote.
2. Rock with olivine completely serpentinized, pyroxenes unaltered or only somewhat altered, and clear plagioclase.
3. Rock with both olivine and the pyroxenes completely to strongly altered, with magnetite mesh in olivine remnants and in altered pyroxenes, with plagioclase usually displaying a milky appearance.
4. Rock with all major minerals serpentinized, bastitized, and plagioclase strongly epidotized; much magnetite.
5. Completely serpentinized rock, translucent, with euhedral late magnetite and pyrite, and no magnetite mesh, with only ghosts or palimpsests of the cumulus minerals.

DATA ON INDIVIDUAL PLATINUM-GROUP MINERALS

Moncheite PtTe$_2$ is the most commonly found mineral in the drill cores studied. Most of the grains are 5 to 20 μm in diameter, but grains of 100 μm are not rare. In almost all cases this mineral occurs in chalcopyrite on the border with silicates and has a roundish habit, with larger grains commonly displaying a typical cleavage, as shown in Figures 2 and 3. Moncheite is more common in monomineralic chal-

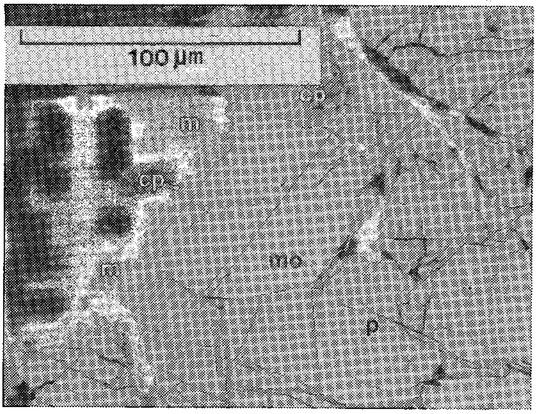

FIG. 2. Moncheite, composition 23/84 and 23/84–1, Frog Pond (Blakely Creek); mo moncheite with cleavage, white; m magnetite, dark grey; cp chalcopyrite, grey; p pentlandite, light grey. Oil immersion, reflected light.

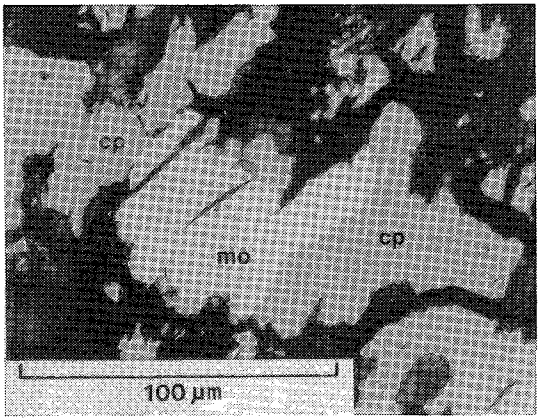

FIG. 3. Moncheite, 30/84–3, Frog Pond (Blakely Creek); mo moncheite, white; cp chalcopyrite, grey. Note typical parting in moncheite. Oil immersion, reflected light.

copyrite grains and veinlet-like aggregates in the immediate vicinity of larger aggregates of sulfide that display a rim of chalcopyrite. Where moncheite is seen in pentlandite and, occasionally, pyrrhotite, it is usually only a few micrometres in diameter, but also roundish. The moncheite at Stillwater is generally pure $PtTe_2$; however, some compositions show insignificant Bi and Sb (Table 2A). With the exception of moncheite from Lac des Iles, Ontario (Cabri & Laflamme 1979, cited in Cabri 1981), moncheite from other localities is usually high in Pd and Bi. Optical data are given in Figure 4. Microhardness VHN_{15} is 135–142, 168–178. The spectral reflectance was measured on six grains; the curves show good agreement, as expected in view of the constant chemistry. The R_1 and R_2 curves obtained are based on a λ of 546 nm: $R_1 = 54.8$, $R_2 = 62.3\%$. These values correspond well with published data of Tarkian & Bernhardt (1984). Somewhat different curves by Cabri (1981) probably reflect a different composition. Owing to its reflectivity, moncheite appears almost metallic white against the sulfides of Cu, Fe and Ni.

Sperrylite $PtAs_2$ is probably the second most abundant mineral. It occurs mostly in silicates, and in relatively small, often clustered anhedral grains, usually varying between 3 to 15 µm, and occasionally up to 40 µm in diameter. Larger grains seem to occur preferentially inside sulfide aggregates as well as in the vicinity of such "blebs". Sperrylite also tends to form stringers of anhedral grains in a vein-like formation in silicates. The composition is remarkably stable (Table 2A). Sperrylite appears white where surrounded by silicates, greyish white to grey where bordering on base-metal sulfides, and commonly shows a peculiar dull surface.

Cooperite, braggite and *vysotskite,* if considered collectively as representatives of the system PtS–PdS–NiS (in spite of the fact that cooperite is not polymorphous with braggite–vysotskite: Cabri *et al.* 1978) would represent the most common minerals at Stillwater. A comprehensive study of these minerals has recently been presented by Criddle &

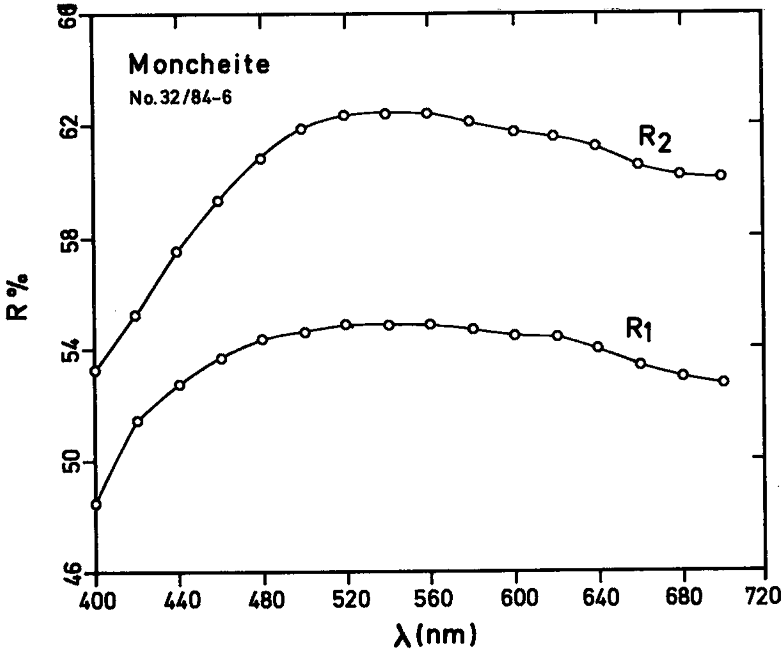

FIG. 4. Reflectance spectra for moncheite.

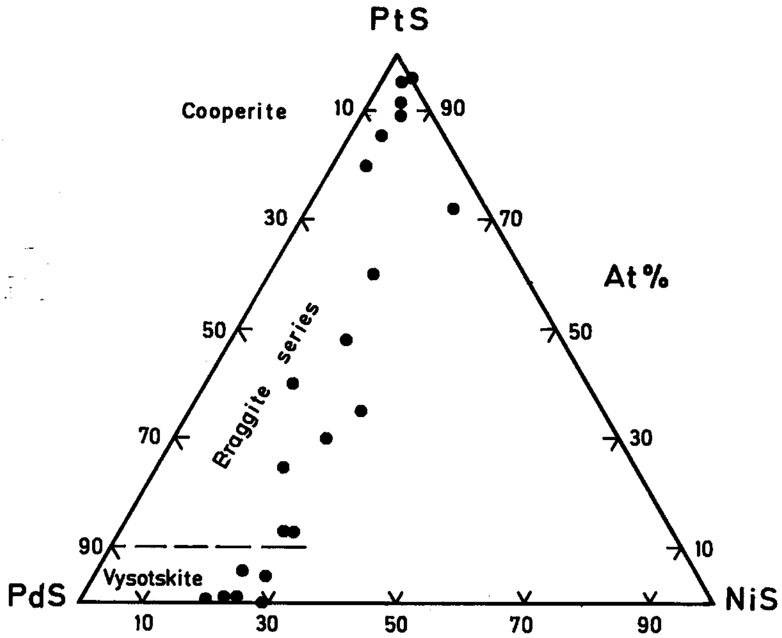

FIG. 5. New compositions of cooperite, braggite and vysotskite from the J-M Reef, plotted in the PtS-PdS-NiS composition triangle.

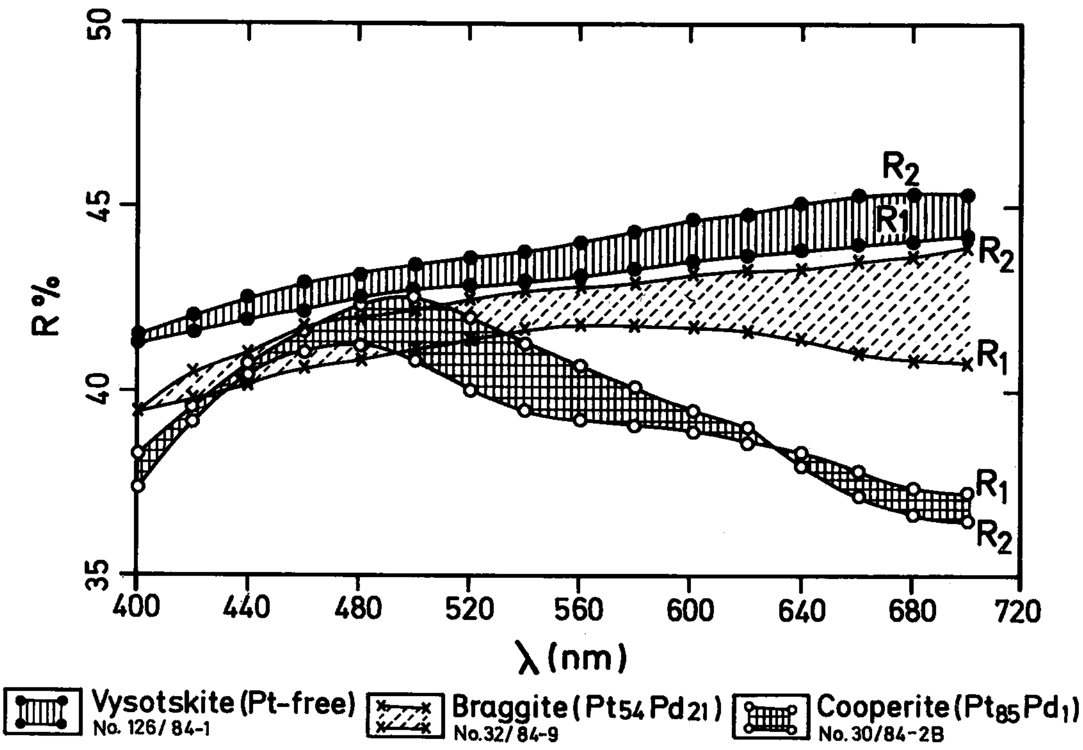

FIG. 6. Reflectance spectra for Pd-poor cooperite, braggite (54 wt.% Pt, 21 wt.% Pd) and Pt-free vysotskite.

Stanley (1985). It appears to us that the abundance of braggite–vysotskite and the palladium content of pentlandite increase somewhat toward the east when one considers also the mineralogy of the West Fork and the Minneapolis adits, not included here because of ongoing studies by A.J. Criddle, C.J. Stanley and C. Bow *et al.* We have so far made preliminary studies of over 100 polished sections from these adits, and are basing the above statement also on our own observations. Twenty-one grains of cooperite and the solid solution vysotskite–braggite were analyzed (Table 2B). The cooperite is Ni-poor and shows from 0 to 8% Pd. The composition of analyzed members of the vysotskite–braggite series varies between $Pt_5Pd_{68}Ni_{27}$ and $Pt_{59}Pd_{24}Ni_{17}$ ($\Sigma = 100$). Four grains of vysotskite are practically Pt-free and fall on the line PdS–NiS (Fig. 5). For reflectance measurements, a grain of Pd-free cooperite, one of Pt-free vysotskite and one of braggite of intermediate composition (54 wt.% Pt, 21% Pd) were chosen (Fig. 6). Accordingly, we obtain different reflectance curves for these minerals.

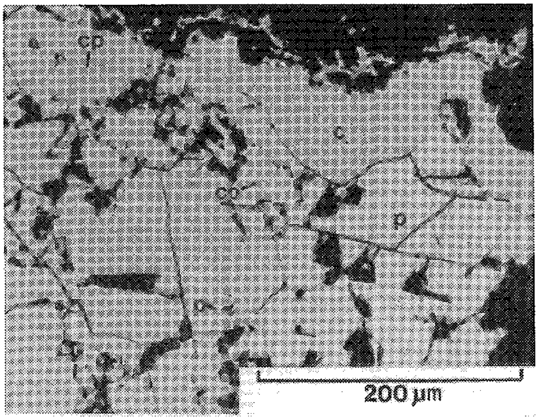

FIG. 7. Cooperite, c, grey; pentlandite, p, white; chalcopyrite, cp, grey; 50/84–3, Frog Pond. Oil immersion, reflected light.

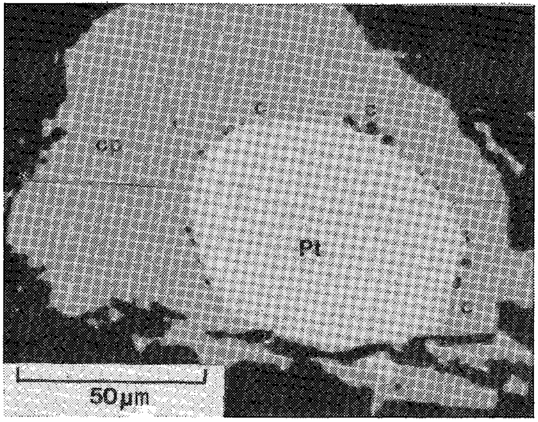

FIG. 8. Round ferroplatinum grain rimmed by cooperite, which is rimmed by chalcopyrite; composition 30/84–3, Frog Pond (Blakely Creek); ferroplatinum, Pt, white; c cooperite rim, light grey; cp chalcopyrite, grey. Oil immersion, reflected light.

Cooperite PtS occurs in roundish grains, usually 10 to 50 µm in diameter (Fig. 7), near chalcopyrite–silicate boundaries in larger, or near larger aggregates of sulfide, but also in pyrrhotite and between chalcopyrite and pyrrhotite grains and rarely between pentlandite and chalcopyrite grains. Next to pentlandite and pyrrhotite, cooperite appears grey, almost resembling magnetite; at chalcopyrite–silicate boundaries it looks quite white and reflectant and could be mistaken for moncheite. The much greater hardness of cooperite and braggite helps to optically distinguish both minerals from moncheite. The reflectance curves for cooperite were measured on several grains; they are similar to those given by Cabri (1981) and Criddle & Stanley (1985). The somewhat different bireflectance is due to difference in orientation of grains chosen for measurement. Reflectance and microhardness data are given in Table 3. The seven compositions of cooperite determined are plotted in the PtS–PdS–NiS composition triangle (Fig. 5) (see also Cabri *et al.* 1978, p. 835).

Cooperite seems to associate closely with the Pt–Fe alloy in Stillwater, forming occasionally a complex rim of single crystals around the metal (Fig. 8), with braggite forming somewhat further toward surrounding chalcopyrite and pyrrhotite and other sulfides. As Cabri *et al.* (1978) pointed out, the assemblage cooperite + isoferroplatinum + pyrrhotite is important, because it is stable at 1000°C, based on the work of Skinner *et al.* (1976).

TABLE 3. OPTICAL DATA FOR COOPERITE, BRAGGITE AND VYSOTSKITE

Sample No.	cooperite 30/84-2B		braggite 32/84-9		vysotskite 126/84-1	
λnm	R_1	R_2	R_1	R_2	R_1	R_2
400	37.4	38.3	39.4	39.6	41.3	41.3
420	39.4	39.5	39.6	40.6	41.6	42.0
440	40.5	40.6	40.7	41.0	42.0	42.4
460	41.0	41.6	40.7	41.6	42.2	42.9
480	41.2	42.2	40.9	42.0	42.5	43.0
500	40.8	42.5	41.3	42.2	42.6	43.5
520	40.0	42.0	41.5	42.5	42.6	43.5
540	39.5	41.3	41.7	42.7	42.9	43.7
560	39.3	40.7	41.8	42.8	43.1	44.0
580	39.2	40.1	41.8	43.0	43.3	44.3
600	39.0	39.4	41.8	43.3	43.5	44.6
620	38.8	38.9	41.7	43.3	43.7	44.7
640	38.3	38.0	41.4	43.3	43.8	45.0
660	37.8	37.2	41.1	43.6	44.0	45.3
680	37.4	36.6	40.9	43.7	44.0	45.3
700	37.4	36.4	41.0	44.0	44.1	45.3
Color values(C)						
x	0.3057	0.3045	0.3124	0.3139	0.3131	0.3141
y	0.3132	0.3169	0.3200	0.3205	0.3186	0.3195
Y%	39.5	40.7	41.6	42.8	43.1	44.0
Pe%	1.9	2.0	1.6	2.2	1.4	1.9
λd	482	492	571	576	580	580
Micro-indentation hardness						
VHN_{35}	730-790				582-630	

Braggite (Pt,Pd)S is more common than cooperite or vysotskite in the polished sections studied. Of all the PGM it forms the largest grains, up to 200 μm, but they are seldom homogeneous. The composition and optical orientation vary greatly in aggregates of polysynthetically twinned braggite (Fig. 9). These tend to occur in larger pentlandite–pyrrhotite–chalcopyrite aggregates near the interface with silicates, but are mostly surrounded by the other sulfides. They appear to have formed later than the pentlandite and pyrrhotite, and commonly have inclusions of chalcopyrite and, locally, pyrite. Owing to very similar qualitative reflectivity and hardness, braggite can be distinguished from cooperite optically only with difficulty; however, it does not seem to occur in the round shapes that the cooperite shows, and tends to be almost interstitial within the sulfide aggregates and quite anhedral in shape. We have not seen the very large idiomorphic, homogeneous grains of braggite described by Criddle & Stanley (1985). Braggite seems to be associated with millerite and sperrylite. Sperrylite commonly is found in the silicates near a larger aggregate of braggite grains, even in the Fe–Ni–Cu sulfides of the host sulfide aggregates. The eight compositions of braggite in Table 2B reflect the variable composition of this mineral in Stillwater. Owing to the inhomogeneity of braggite grains, accurate measurements of reflectance and hardness are difficult. Therefore, reflectance of only one intermediate homogeneous grain was measured (Fig. 6). The braggite compositions along the reef are plotted in the PtS–PdS–NiS triangle with cooperite and vysotskite (Fig. 5).

Vysotskite (Pd,Ni,Pt)S is less common than braggite and cooperite. It occurs in relatively small elongate grains, 10–30 μm in diameter, mainly in sulfides near the rim of sulfide aggregates, or in silicates still attached to a sulfide, mainly pentlandite or pyrrhotite. The Ni contents (Table 2B) are higher than those reported by Criddle & Stanley (1985) for Pt-bearing vysotskite. Specifically, it seems to be common in the vicinity of millerite, and where the latter replaces pentlandite, then vysotskite is commonly surrounded by millerite. Heazlewoodite also appears in these aggregates. Oxidation of primary sulfides and replacement by magnetite are frequently the typical assemblages for vysotskite. In addition to relatively homogeneous grains carrying little or no platinum, vysotskite compositions were encountered in a large inhomogeneous aggregate of braggite–vysotskite, surrounded by millerite (Fig. 10). This grain shows a much wider compositional variation than revealed in the two compositions given here. More details are given in Volborth (1985). Six vysotskite compositions are given in Table 2B. The spectral reflectance curves, as well as microhardness, were measured for selected analyzed spots in this grain as well as in a couple of small homogeneous grains (Table 3).

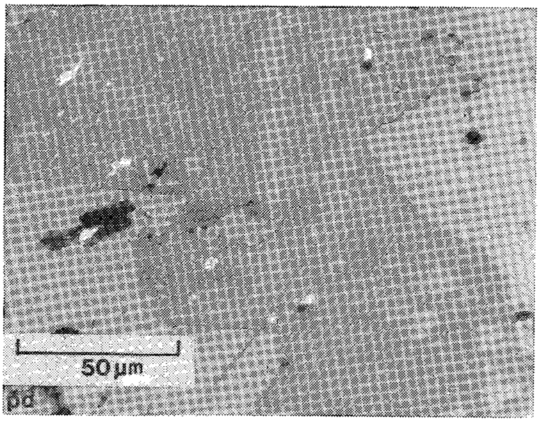

FIG. 9. Braggite, polysynthetically twinned, 15/84, Frog Pond (Blakely Creek); partly crossed nicols. The whole area is braggite; only in one corner is there a little pentlandite, pd. Oil immersion, reflected light.

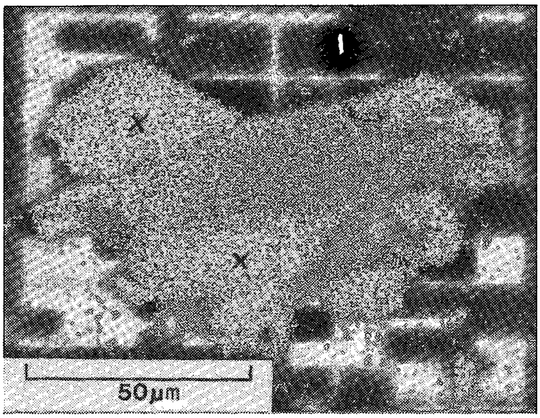

FIG. 10. Palladium distribution in a heterogeneous vysotskite–braggite crystal, compositions 1/81–1, 1/81–2, Iron Mountain. X-ray scan. Location of spot-analyses marked with crosses.

The curves shown in Figure 6 can be considered representative for Pt-free vysotskite and are comparable to those measured by Criddle & Stanley (1985). The calculated values of color are given in Table 3. Vysotskite is anisotropic. Before the recent work by Criddle & Stanley (1985), only a single middle-reflectance curve by Vyal'sov (1973), used by Cabri (1981), existed. These early data differ considerably from our measurements. Vyal'sov does not give a chemical composition. Our measurements (Table 3) show that the microhardness of Pt-free vysotskite is lower than that of cooperite and somewhat lower than that reported by Criddle & Stanley (1985) for Pt-bearing vysotskite.

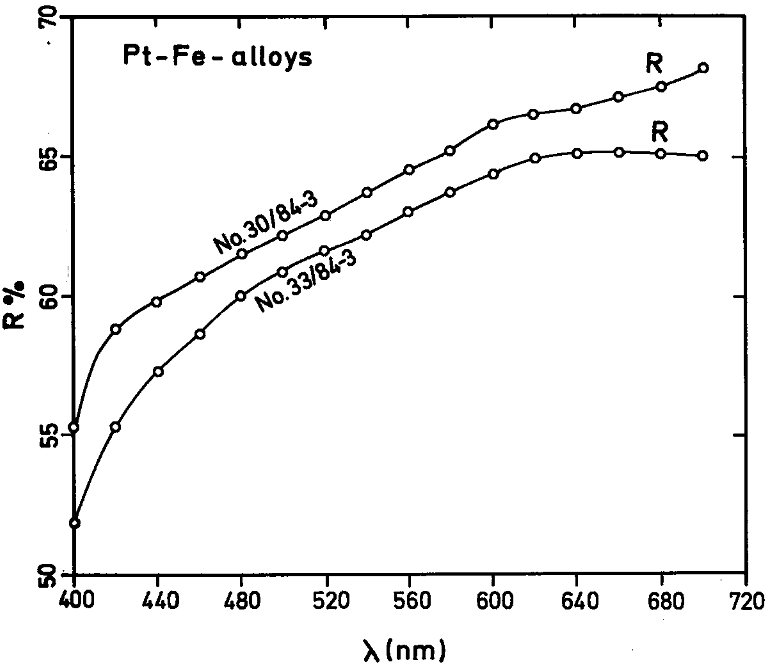

FIG. 11. Reflectance spectra of Pt-Fe alloys, No. 30/84-3: 10.7 wt.% Fe, 4.8 wt.% Pd; No. 33/84-3: 10.2 wt.% Fe, 0.4 wt.% Pd.

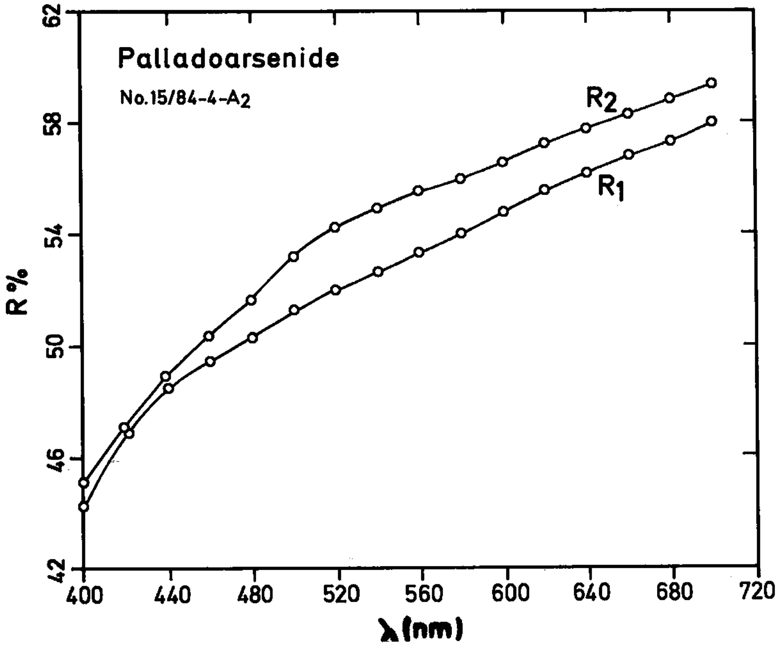

FIG. 12. Reflectance spectra of palladoarsenide.

A *Pt-Fe alloy* is relatively common; it generally occurs in very small grains approximately 5 μm across, usually in clusters, or worm-like aggregates, rarely as larger, 10–50 μm, rounded or irregular grains, then occasionally surrounded by cooperite-braggite and chalcopyrite (Fig. 8) (see cooperite). The Pt-Fe alloy seems to appear mainly in strongly serpentinized parts of the deposits. Two spectral reflectance curves are given in Figure 11. Measured microhardness VHN_{30} on analyzed Pt-Fe is 310–321 (for composition see Table 2B). Note that the Pd-bearing grains show 2–3% higher reflectance at the same Fe-content. Ten compositions with formulae are given in Table 2B. Most show a few percent palladium, but the composition remains remarkably consistent along the reef. Ni is present only in traces. Cabri & Laflamme (1974) also emphasized the consistency in composition of the three Pt-Fe grains from concentrates that they studied.

Palladoarsenide Pd_2As is rare; it occurs in two small elongate grains 10–30 μm across, near larger aggregates of sulfide rich in pentlandite and pyrrhotite rimmed by chalcopyrite. Sperrylite is then usually abundant in the sulfide aggregates as well as in silicates in the immediate vicinity. Compositions in Table 2A correspond to stoichiometric palladoarsenide. Unlike the two grains of palladoarsenide described by Cabri *et al.* (1975), the grain found was suitable for measurement of reflectance (Fig. 12) and microhardness (VHN_{10} 289–331), thus permitting us to obtain data complementary to those compiled by Tarkian & Bernhardt (1984). To our knowledge, the only other published optical data on this mineral are provided by Begizov *et al.* (1974), and the color values are given by us for the first time (Table 4).

TABLE 4. OPTICAL DATA FOR KEITHCONNITE AND PALLADOARSENIDE

Sample No.	keithconnite 13/84-3		palladoarsenide 15/84-4-A2	
λnm	R_1	R_2	R_1	R_2
400	40.8	40.6	44.2	45.1
420	41.6	41.1	46.8	46.8
440	41.8	41.5	48.4	48.8
460	42.0	42.0	49.4	50.3
480	42.3	42.6	50.2	51.6
500	42.9	43.4	51.2	53.1
520	43.6	44.1	51.9	54.1
540	44.4	44.9	52.5	54.8
560	45.3	45.8	53.3	55.4
580	46.0	46.6	53.9	55.8
600	46.8	47.5	54.6	56.3
620	48.0	48.8	55.4	57.1
640	49.3	49.9	56.0	57.6
660	50.6	50.9	56.6	58.1
680	52.0	52.1	57.1	58.6
700	53.5	53.4	57.8	59.2
Color values(C)				
x	0.3215	0.3227	0.3200	0.3208
y	0.3235	0.3253	0.3254	0.3284
Y%	45.2	45.8	53.1	55.1
Pe%	5.0	5.8	5.1	6.1
λd	584	582	579	576
Micro-indentation hardness VHN_{10}	-		289-331	

Stillwaterite Pd_8As_3 in its type locality (Cabri *et al.* 1975) occurs as a single anhedral grain, near pentlandite and pyrrhotite with palladoarsenide, along with sperrylite grains and a large grain of braggite (>200 μm), in a sulfide aggregate rimmed by chalcopyrite. The analytical data reveal a remarkably stoichiometric composition (Table 2A) compared to the 13 grains of stillwaterite analyzed by Cabri *et al.* (1975). Our first EMP data indicated a composition closer to guanglinite, Pd_3As.

Keithconnite $Pd_{3-x}Te$ in its type locality (Cabri *et al.* 1979) occurs as two small grains 15 μm across in silicates near disseminated grains of chalcopyrite in association with moncheite, vysotskite, gold and palladian pentlandite. Despite the small grain-size, it was

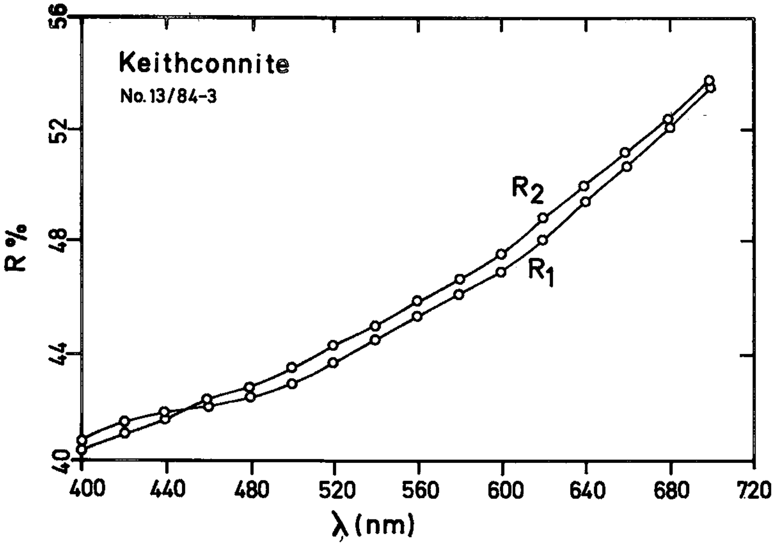

FIG. 13. Reflectance spectra of keithconnite.

possible to obtain a useful analysis (Table 2A), as well as spectral reflectance data (Fig. 13, Table 4). Keithconnite shows a weak anisotropy and low bireflectance.

Kotulskite PdTe occurs in one polished section, not yet sufficiently described, from western Frog Pond, in association with sperrylite, pentlandite, pyrrhotite, chalcopyrite and late pyrite. Its composition is given in Table 2A.

Four grains of *hollingworthite* RhAsS are found closely associated with cobaltite, (Au,Ag), pyrrhotite, pentlandite, pyrite and chalcopyrite (Figs. 14, 15, 16). Composition (no. 14/84-6): Rh 35.2, Pt 10.6, Pd 7.1, Ir 0.1, As 35.0, S 12.7, Σ100.7%. Formula: $(Rh_{0.77}Pd_{0.15}Pt_{0.12}Ir_{0.01})_{\Sigma 1.05}As_{1.05}S_{0.90}$.

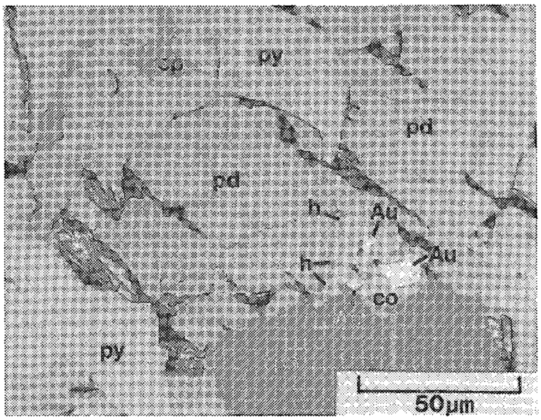

FIG. 14. Hollingworthite, h, Blakely Creek, cluster of crystals in cobaltite, co, with three (Au,Ag) grains, white, in a sulfide aggregate with pyrrhotite po, pentlandite pd, pyrite py and chalcopyrite cp. Oil immersion, reflected light. See Figures 15 and 16 for distribution of Rh and Ir.

The grains are too small and too inhomogeneous for reflectance and hardness measurements. This is the first published composition of this mineral at Stillwater; Cabri only mentions this mineral as occurring in the Stillwater complex (1981, p. 239). Tarkian & Stumpfl (1975) described hollingworthite first from the Driekop mine in Transvaal. In North America, it is mentioned as occurring at Werner Lake, Ontario (Rucklidge 1969). The other locality known is Hitura, Finland (Häkli *et al.* 1976). It appears that hollingworthite occurs quite commonly at Stillwater with gold, braggite and sperrylite, as a thin crust around other Pt–Pd minerals and as minute inclusions in these. Of interest are iridium-rich flame-like inclusions in the three crystals of hollingworthite pictured in Figures 15 and 16. Cabri *et al.* (1984) reported between 60 and 112 ppm Rh in the pentlandite from Stillwater.

Electrum (Au,Ag) is quite abundant and tends to occur surrounded by silicates or in close association with cobaltite (Figs. 14, 15) and FeNi- and Ni-sulfides where magnetite is present. It appears to evolve in serpentinized regions as a secondary mineral. Composition: Au 84.5, Ag 14.6%, formula: $Au_{0.76}Ag_{0.24}$.

A CuZnFeSn *alloy* occurs in veinlets and numerous minute grains, 5 µm across, as a secondary mineral with marcasite, pyrite, graphite, epidote and serpentine in one polished section. Composition: Cu 85.0, Zn 5.5, Sn 2.7, Fe 2.9%.

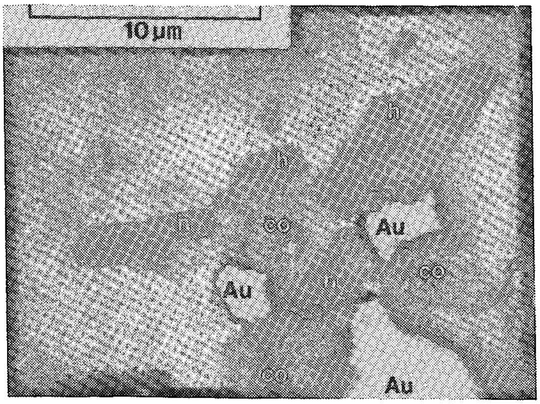

FIG. 15. Electron back-reflection scan showing the distribution of iridium in the hollingworthite crystals shown in Figure 14, h, grey; (Au,Ag), white, and the cobaltite cluster, co. Note the lighter Ir-rich plume in centre of the three crystals of hollingworthite.

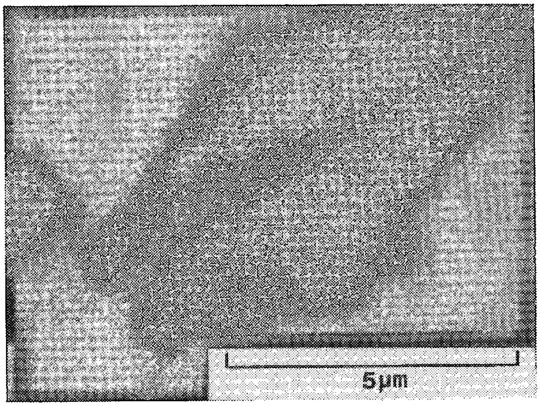

FIG. 16. Rhodium X-ray scan of the largest crystal of hollingworthite, h, in Figures 14 and 15. Iridium is concentrated in a plume-like dark zone diagonally across the crystal. Compare with Figure 15, where iridium electron backscatter is strongest within each of the three crystals of hollingworthite, owing to an iridium-rich zone in the centre.

NEW DATA ON THE GRAPHITE-RICH COARSE PYROXENITES

Michenerite PdBiTe occurs in the Janet-50 graphite-rich zone under the reef (Volborth & Housley 1984). Here it is in association with hessite AgTe, wehrlite BiTe (see Hoffman & MacLean 1976, who described a very similar experimental paragenesis for a temperature range of 380° to 490°C), sphalerite, magnetite, pentlandite, chalcopyrite, pyrrhotite, niccolite, cobaltite, major graphite, and an alloy, BiNi, not previously described as a mineral but known in metallurgy (Hansen 1958). We have not seen michenerite in the main PGE zone. Results of a scanning-electron-microscope (SEM) analysis of this michenerite are given in Table 2A.

Of interest is the occurrence in these graphite-rich pyroxenite pegmatoids of originally euhedral, partly resorbed *chlorapatite,* of which two grains gave by nondispersive SEM analysis: Ca 40.0, P 17.5, Cl 5.4 and Fe 1.8%, and Ca 39.9, P 17.5, Cl 6.3 and Fe 1.9%. The massive graphite of this pegmatoid also contains in most cases at least a few tenths of one percent chlorine (>0.1%). The presence of major Cl could explain the separation of Pt complexed with chlorine from Pd in these and similar deposits. We have here in mind the separate occurrence of the main Pt minerals moncheite, cooperite and sperrylite in the vicinity of palladian pentlandite, vysotskite, and the rarer palladium tellurides and arsenides. We believe that Pt could have separated from palladium in early stages in the form of chloride complexes, later reacting with sulfur and arsenic. Tapani Mutanen, of the Finnish Geological Survey, has recently also discovered cumulus chlorapatite at Koitelainen, in Finnish Lapland (priv. comm., 1985). Chlorapatite has been previously reported by Volborth & Housley (1984) from the Janet claims and by Boudreau & McCallum (1985) from the pegmatoid J-M Reef near Picket Pin in Stillwater. Boudreau & McCallum emphasized that whereas the chlorine content of apatite from the Anorthosite II zone is similar to that of other layered intrusive complexes, the chlorine content of the reef's apatite is unusually high. The importance of the Cl has been also emphasized for the Bushveld Complex by Schiffries (1982) and Kinloch (1982).

In addition, the unusual assemblage described includes small grains of rare-earth minerals, a Th mineral, Sc- and Y-rich minerals, calcite, quartz and chromian phlogopite mica rich in Cl (see Boudreau & McCallum 1985).

Of exceptional interest in the above association with graphite is the occurrence of four grains of a *rhenium sulfide* Re_2S_3 in a pentlandite-pyrrhotite aggregate in graphite-rich coarse pyroxenite. This assemblage is to be described in more detail in a separate paper. In none of the hundreds of polished sections examined have we seen molybdenite. This, and the appearance of a Re mineral, should indicate the dearth of Mo in these Stillwater PGE ores.

DISCUSSION AND CONCLUSIONS

In this work, we attempt to present a description of the PGE mineralogy and to relate the compositional changes along the whole strike-length of the J-M Reef. New data on the pyroxenite pegmatoid graphitic layers some 200 m below the J-M Reef give this work some three-dimensional scope. The information here given represents less than 10% of the material studied in polished section. The amount of information is so overwhelming that only the most important data are compiled. We had to abandon many original concepts as materials accumulated (see Open-File Report, Volborth 1985) and we do realize that this work is only a very preliminary pilot study of the core material available to us. Therefore, at this stage we have avoided comparisons with recent, and already classic, mineralogical studies of the Merensky Reef and the UG-2 chromitite by Vermaak & Hendriks (1976), McLaren & DeVilliers (1982), Kingston & El-Dosuky (1982), Mostert *et al.* (1982), Kinloch (1982) and Peyerl (1982), and with that of the Noril'sk Cu-Ni deposits by Genkin *et al.* (1981). Without doubt these studies have significantly influenced our planning, our thinking, and thus the overall structure and nature of this work, but it is too early to enter into protracted discussion of the genesis of these deposits. Nevertheless, our findings seem to warrant a statement that the abundance of Cl in apatite and graphite may explain the separation of Pd and Pt in the Stillwater and other deposits.

The widespread occurrence of graphite below the J-M Reef points to carbon as an integral constituent of the fluid system that played a significant role in the formation of the Stillwater Reef, and of pegmatites at lower stratigraphic levels. The physicochemical parameters of graphite formation in the Upper Critical Zone of the Bushveld Complex have recently been evaluated by Ballhaus & Stumpfl (1985). Graphite deposition and release of H_2O are linked *via* the reaction $CO_2 + CH_4 = 2C + 2\,H_2O$, and this explains the common association of graphite with hydrous silicates. Chlorine is an important minor constituent in graphite, which thus joins hydrous silicates and apatite as major repositories of chlorine.

The occurrence of rhodium minerals means that not all the Rh in Stillwater is in solid solution in pentlandite, as seems to be the case in the Merensky Reef (Kinloch 1982). The concentration of Pt-Fe alloys in serpentinized rock speaks for their late, secondary nature. There seems to be an increase in frequency of Pd minerals compared to Pt minerals toward the east, when one takes the mineralogy of the West Fork and the Minneapolis adits (not described here) into account. The remarkable consistency in composition of the Pt minerals moncheite, sperrylite, cooperite and the Pt–Fe alloys seems to speak for efficient separation of Pt from Pd at an early stage into different phases owing to the early presence of Cl and S. Replacement phenomena are more advanced in the east of the deposit, as manifested by alteration and increased Pd-mineralization, leading to extremely Pd-rich pentlandite found at the Minneapolis adit. We have studied about 100 polished sections from the Minneapolis adit; the preliminary data of this study are not published here, because a major study of Minneapolis mineralogy by others may be in progress. Also, because minerals from the West Fork adit have been extensively described by Cabri and coworkers, we have left that segment of the Stillwater mineralogy virtually untouched. The frequency of our data is biased toward the Frog Pond section; nevertheless our knowledge of the mineralogy of the Minneapolis and West Fork adits tends to support our contention that palladium mineralization may be more pronounced toward the east.

ACKNOWLEDGEMENTS

This work would not have been possible without devoted major help in selection, cutting and curatorial assistance by Ms. Mariann Prewett of Absarokee, Montana. For permission to collect and cut the drill-core material, we thank Mr. J.M. Sharratt, and for assistance in locating and selecting the material, Dr. E.L. Mann, both of the Manville Corporation. L.J. Cabri has kindly provided us with several PGE standards for the EMP analyses. We are greatly indebted to Mrs. B. Cornelisen of Hamburg and Mr. H. Mühlhans of Leoben, respectively, for expert EMP analyses. Dr. H.J. Bernhardt, of Hamburg, kindly solved some problems with the new Cameca EMP, just installed. Discussions with C.G. Ballhaus of Leoben have reinforced our concept of the genetic importance of Cl in these deposits, based on his unpublished fluid-inclusion studies. We are particularly indebted to R. F. Martin and B. F. Leonard for improvements to the text. We are thankful for the starter grant to one of us (A.V.) by the Montana College of Mineral Science and Technology of Butte, Montana. This grant permitted some travel necessary in order to co-ordinate work at four different institutions. The University of Hamburg, the Mining University of Leoben, the Rockwell International Science Center of Thousand Oaks and the Deutsche Forschungsgemeinschaft have also significantly contributed financially to this study. For typing and setting up of tables, we are indebted to Mrs. Martha J. Schatzka, of Butte; for technical help with maps, scales, photos as well as fruitful discussions, we thank accelerator operator Mr. J.P. Dahy, also of Butte. The contribution of R.M.H. was supported by NASA contract NAS9-11539. The initial support for this work came from NSF grant EAR-821-3044.

REFERENCES

BALLHAUS, C.G. & STUMPFL, E.F. (1985): Occurrence and petrological significance of graphite in the Upper Critical Zone, western Bushveld Complex, South Africa. *Earth Planet. Sci. Lett.* **74**, 58-68.

BEGIZOV, V.D., MESHCHANKINA, V.I. & DUBAKINA, L.S. (1974): Palladoarsenide, Pd_2As, a new natural palladium arsenide from the copper–nickel ores of the Oktyabr deposits. *Int. Geol. Rev.* **16**, 1294-1297.

BOUDREAU, A.E. & MCCALLUM, I.S. (1984): The Picket Pin Pt/Pd zone, Stillwater Complex, Montana. *Lunar Planet. Sci.* **XV**(1), 78-79 (abstr.).

_____ & _____ (1985): Composition of apatite and biotite from the Stillwater Complex, Montana: evidence for hyrothermal transport of PGE and REE in Cl-bearing solutions. *Lunar Planet. Sci.* **XVI**(1), 85-86 (abstr.).

BOW, C., WOLFGRAM, D., TURNER, A., BARNES, S., EVANS, J., ZDEPSKI, M. & BOUDREAU, A. (1982): Investigations of the Howland Reef of the Stillwater Complex, Minneapolis Adit area: stratigraphy, structure, and mineralization. *Econ. Geol.* **77**, 1481-1492.

CABRI, L.J., ed. (1981): *Platinum-Group Elements: Mineralogy, Geology, Recovery.* Can. Inst. Mining Metallurgy, Spec. Vol. **23**.

_____, BLANK, H., EL GORESY, A., LAFLAMME, J.H.G., NOBILING, R., SIZGORIC, M.B. & TRAXEL, K. (1984): Quantitative trace-element analyses of sulfides from Sudbury and Stillwater by proton microprobe. *Can. Mineral.* **22**, 521-542.

_____, CHEN, T.T., STEWART, J.M. & LAFLAMME, J.H.G. (1976). Two new palladium–arsenic–bismuth minerals from the Stillwater Complex, Montana. *Can. Mineral.* **14**, 410-413.

_____, CLARK, A.M. & CHEN, T.T. (1977): Arsenopalladinite from Itabira, Brazil and from the Stillwater Complex, Montana. *Can. Mineral.* **15**, 70-73.

_____ & LAFLAMME, J.H.G. (1974): Rhodium, platinum and gold alloys from the Stillwater Complex. *Can. Mineral.* **12**, 399-403.

_____, _____, STEWART, J.M., ROWLAND, J.F. & CHEN, T.T. (1975): New data on some palladium arsenides and antimonides. *Can. Mineral.* **13**, 321-335.

———, ———, ———, TURNER, K. & SKINNER, B.J. (1978): On cooperite, braggite and vysotskite. *Amer. Mineral.* **63**, 832-839.

______, ROWLAND, J.F., LAFLAMME, J.H.G. & STEWART, J.M. (1979): Keithconnite, telluropalladinite and other Pd–Pt tellurides from the Stillwater Complex, Montana. *Can. Mineral.* **17**, 589-594.

CONN, H.K. (1979): The Johns–Manville platinum–palladium prospect, Stillwater Complex, Montana, U.S.A. *Can. Mineral.* **17**, 463-468.

CRIDDLE, A.J. & STANLEY, C.J. (1985): Characteristic optical data for cooperite, braggite and vysotskite. *Can. Mineral.* **23**, 149-162.

CZAMANSKE, G.K. & ZIENTEK, M.L., eds. (1985): The Stillwater Complex, Montana: geology and guide. *Montana Bur. Mines Geol., Spec. Publ.* **92.**

GENKIN, A.D., DISTLER, V.V., GLADYSCHEV, G.D., FILIMONOVA, A.A., EVSTIGNEEVA, T.L., KOVALENKER, V.A., LAPUTINA, I.P., SMIRNOV, A.V. & GROKHOVSKAYA, T.L. (1981): Copper–Nickel Sulfide Ores of Noril'sk. *Nauka, Moscow* (in Russ.).

HÄKLI, T.A., HÄNNINEN, E., VUORELAINEN, Y. & PAPUNEN, H. (1976): Platinum group minerals in the Hitura nickel deposit, Finland. *Econ. Geol.* **71**, 1206-1213.

HANSEN, M. (1958): *Constitution of Binary Alloys.* McGraw-Hill, New York.

HOFFMAN, E. & MACLEAN, W.H. (1976): Phase relations of michenerite and merenskyite in the Pd–Bi–Te system. *Econ. Geol.* **71**, 1461-1468.

KINGSTON, G.A. & EL-DOSUKY, B.T. (1982): A contribution on the platinum-group mineralogy of the Merensky Reef at the Rustenburg platinum mine. *Econ. Geol.* **77**, 1367-1384.

KINLOCH, E.D. (1982): Regional trends in the platinum-group mineralogy of the Critical Zone of the Bushveld Complex, South Africa. *Econ. Geol.* **77**, 1328-1347.

MCCALLUM, I.S., RAEDEKE, L.D. & MATHEZ, E.A. (1980): Investigations of the Stillwater Complex. I. Stratigraphy and structure of the banded zone. *Amer. J. Sci.* **280-A**, 59-87.

MCLAREN, C.H. & DEVILLIERS, J.P.R. (1982): The platinum group chemistry and mineralogy of the UG–2 Chromitite layer of the Bushveld Complex. *Econ. Geol.* **77**, 1348-1366.

MOSTERT, A.B., HOFMEYR, P.K. & POTGIETER, G.A. (1982): The platinum group mineralogy of the Merensky Reef at the Impala platinum mines, Bophuthaswana. *Econ. Geol.* **77**, 1385-1394.

PAGE, N. J (1971): Sulfide minerals in the G and H chromitite zones of the Stillwater Complex, Montana. *U.S. Geol. Surv., Prof. Pap.* **694.**

______ (1979): Stillwater Complex, Montana – structure, mineralogy and petrology of the Basal zone with emphasis on the occurrence of sulfides. *U.S. Geol. Surv. Prof. Pap.* **1038.**

______, ZIENTEK, M.L., CZAMANSKE, G.K. & FOOSE, M.P. (1985): Sulfide mineralization in the Stillwater Complex and underlying rocks. *In* the Stillwater Complex, Montana: Geology and Guide (G.K. Czamanske & M.L. Zientek, eds.). *Montana Bur. Mines Geol., Spec. Publ.* **92**, 93-96.

PEYERL, W. (1982): The influence of the Driekop dunite pipe on the platinum-group mineralogy of the UG–2 chromitite in its vicinity. *Econ. Geol.* **77**, 1432-1438.

RUCKLIDGE, J. (1969): Electron microprobe investigations of platinum metal minerals from Ontario. *Can. Mineral.* **9**, 617-628.

SCHIFFRIES, C.M. (1982): The petrogenesis of a platiniferous dunite pipe in the Bushveld Complex: infiltration metasomatism by a chloride solution. *Econ. Geol.* **77**, 1439-1453.

SKINNER, B.J., LUCE, F.D., DILL, J.A., ELLIS, D.E., HAGAN, H.A., LEWIS, D.M., ODELL, D.A., SVERJENSKY, D.A. & WILLIAMS, N. (1976): Phase relations in ternary portions of the system Pt–Pd–Fe–As–S. *Econ. Geol.* **71**, 1469-1475.

TARKIAN, M. & STUMPFL, E.F. (1975): Platinum mineralogy of the Driekop mine, South Africa. *Mineral. Deposita* **10**, 71-85.

______ & BERNHARDT, H.J. (1984): A key diagram for the optical determination of platinum group minerals. *Tschermaks Mineral. Petrog. Mitt.* **33**, 121-129.

TODD, S.G., KEITH, D.W., LEROY, L.W., SCHISSEL, D.J., MANN, E.L. & IRVINE, T.N. (1982): The J–M platinum–palladium Reef of the Stillwater Complex, Montana. I. Stratigraphy and petrology. *Econ. Geol.* **77**, 1454-1480.

VERMAAK, C.F. & HENDRIKS, L.P. (1976): A review of the mineralogy of the Merensky Reef, with specific reference to new data on the precious metal mineralogy. *Econ. Geol.* **71**, 1244-1269.

VOLBORTH, A. (1984): Graphite, sulfide, arsenide, rhenium and platinoid mineralization in a pegmatoid pyroxenite of the Stillwater Complex, Montana. *27th Int. Geol. Congress (Moscow)* **IX(2)**, 179-180 (abstr.)

______ (1985): Sulfide and associated platinoid mineralization in the Stillwater "Reef" and underlying graphite-pyroxenite pegmatoids: *Montana Bur. Mines Geol. Open-File Report* **161.**

_____ & HOUSLEY, R.M. (1983): Complex graphite, sulfide, arsenide, palladium and platinum mineralization in a pegmatoid pyroxenite of the Stillwater Complex, Montana. *Lunar Planet. Sci.* **XIV,** 802-803 (abstr.).

_____ & _____ (1984): A preliminary description of complex graphite, sulfide, arsenide, and platinum group element mineralization in a pegmatoid pyroxenite of the Stillwater Complex, Montana, U.S.A. *Tschermaks Mineral. Petrog. Mitt.* **33,** 213-230.

VYAL'SOV, L.N. (1973): *Reflection Spectra of Ore Minerals.* Acad. Sci. USSR, Inst. Geol. of Ore Deposits, Moscow (in Russ.).

WOLFGRAM, D. & EVANS, J.C. (1980): Platinum group mineral and base metal sulfide phase relationships in the "Main platiniferous Zone" of the Stillwater Complex, Montana. *Geol. Soc. Amer., Abstr. Programs* **12,** 552.

Received August 4, 1985, revised manuscript accepted November 13, 1985.